

ELASTIC SCATTERING OF $d\mu$ MESIC ATOMS ON PROTONS, DEUTERONS, AND COMPLEX NUCLEI

V. P. DZHELEPOV, P. F. ERMOLOV, V. I. MOSKALEV, V. V. FIL'CHENKOV, and M. FRIML

Joint Institute for Nuclear Research

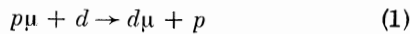
Submitted to JETP editor May 13, 1964

J. Exptl. Theoret. Phys. (U.S.S.R.) 47, 1243-1256 (October, 1964)

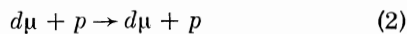
Further experiments on the kinetics of $d\mu$ atomic processes are described. The range distributions of $d\mu$ atoms in hydrogen containing various concentrations of deuterium and of Z-impurities (C, O) and the heretofore unknown cross sections for elastic scattering of $d\mu$ atoms were measured, using a diffusion chamber in a magnetic field. The cross sections were determined by a χ^2 comparison of the experimental distributions with those calculated by the Monte Carlo method. The elastic scattering cross sections (given in Table IV) agree well with the theory. The lifetime of the $d\mu$ atom in hydrogen gas containing Z-impurity concentrations of $1/4000$ and $1/800$ is 1.25 ± 0.16 and 0.42 ± 0.05 μ sec, respectively.

1. INTRODUCTION

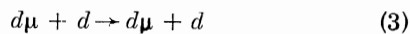
IT is known that after negative muons have stopped in hydrogen and formed mesic atoms various meso-atomic and mesomolecular processes can occur. It has been shown experimentally [1] that in liquid hydrogen having natural deuterium contamination $d\mu$ atoms are produced because of the high rate of the exchange reaction



The range of this kind of mesic atom can be observed as a small displacement (~ 1 mm) of the muon-decay electron track from the muon ending. Such displacements are not observed with as much as $\sim 1\%$ deuterium concentration. This effect is accounted for qualitatively by the theory in [2,3], which derives an anomalously small cross section for the elastic scattering of $d\mu$ atoms on protons:



whereas a relatively large cross section is obtained for scattering on deuterons:



We observed much longer $d\mu$ ranges (~ 10 mm) with a low hydrogen density in the diffusion chamber, and this effect was used to determine the rate of reaction (1). [4,5]

The present work was undertaken to determine quantitatively the experimental cross sections for (2) and (3) by analyzing the distributions of the $d\mu$ ranges and comparing them with theoretical pre-

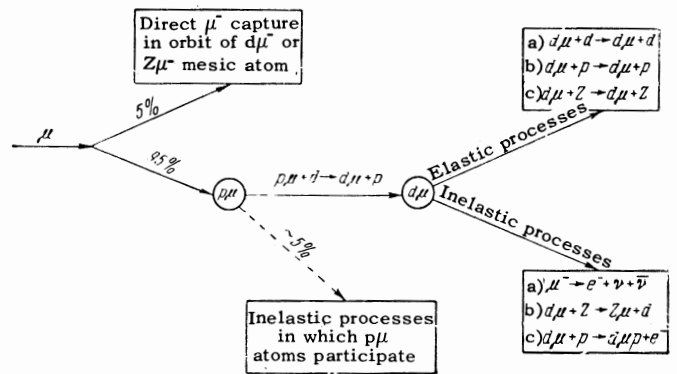


FIG. 1. Scheme of processes participated in by $d\mu$ atoms in a 95% H + 5% D mixture.

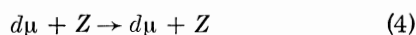
dictions. In these experiments the diffusion chamber was filled with hydrogen containing a small amount ($\sim 5\%$) of deuterium. Figure 1 shows the scheme of processes in which $d\mu$ atoms participate. A $d\mu$ atom produced in reaction (1) possesses an energy of about 45 eV ($1/3$ of 135 eV, which is about the energy difference between the 1s states of $d\mu$ and $p\mu$ atoms). A $d\mu$ atom loses its energy through elastic collisions with protons, deuterons, and complex nuclei (C and O nuclei in the alcohol used as the working liquid of the chamber), until some "inelastic" process occurs, as a result of which the mesic atom ceases to exist. These inelastic processes are: a) muon decay from the $d\mu$ orbit (decay rate $\lambda_0 = 0.45 \times 10^6$ /sec); b) muon transfer from a deuteron to a complex nucleus (rate λ'_{ZCZ}); c) production of $p d\mu$ mesic molecules at the rate $\lambda'_{pd\mu}$ followed by the catalysis

Table I

Experiment	H + D pressure, atm	c_D , %	Working liquid	Combined C and O concentration, %	Number of photographs	Muon stop count	Number of measured events	Final number of events	
1	23.0	4.3	CH ₃ OH	$0,125 \pm 0,030$	50310	12500	1465	1029	
2		6.7			52950	15160	916	623	
3		6.7	C ₃ H ₇ OH		$0,025 \pm 0,006$	38680	8430	1114	937
4		5.6				17070	4120	405	405
5		22.7	0.44		CH ₃ OH	$0,125 \pm 0,030$	10100	1220	341
Σ^*					169110	41430	4241	3267	
Schiff experiment [7]	Liquid H ₂	0,04	Neon atom concentration	$1,8 \times 10^{-2}$ %		28068	68	68	

*Sum over all experiments.

of nuclear reactions in this mesic molecule. The combined rate of "inelastic" processes $\lambda = \lambda_0 + \lambda_Z^c Z + \lambda_{pd}^d \mu$ determines the $d\mu$ lifetime, and together with the cross sections for the elastic processes (2), (3), and



determines the total range, in the gas, of a $d\mu$ atom until it decomposes.

Our present method of analysis and the study of elastic processes enabled us to determine independently the lifetime of the $d\mu$ atom in hydrogen gas, and thus to refine the data on the transfer rate (λ_Z^d) of muons from deuterons to complex impurity atoms. Knowledge of the kinetics of the $d\mu$ interactions studied here is also important for interpreting our data on the yields of catalytic nuclear reactions in hydrogen gas. [5,6]

2. EXPERIMENTAL CONDITIONS AND STUDY OF PHOTOGRAPHS

The diffusion chamber of 380 mm diameter in a 7000-Oe magnetic field was exposed to a negative muon beam slowed by a filter and stopping in the gas of the chamber. We have previously [4-6] given a detailed description of the experimental scheme and conditions using a meson beam from the synchrocyclotron of the Joint Institute for Nuclear Research.

In order to determine how the different relative contributions of elastic processes (2)-(4) and of inelastic processes influenced the $d\mu$ range distribution, five experiments were performed with different concentrations of deuterium and of C and O nuclei in the hydrogen filling the chamber. In all cases the combined hydrogen and deuterium pressure was about 23 atm. The deuterium concentration in the chamber was determined from its partial pressure and was known with at most 4% error. Table I contains the main data from these experiments.

In experiments 1, 2, and 5 the working liquid of the chamber was methyl alcohol, with a 8-sec working cycle. In order to reduce the concentration of C and O atoms in the vapor of the working liquid, the methyl alcohol was replaced in experiments 3 and 4 by normal propyl alcohol C₃H₇OH, but the temperature regime of the chamber remained the same as in experiments 1, 2, and 5. At -18°C, which is the temperature at the upper boundary of the sensitive layer in the chamber, the pressure of saturated propyl alcohol vapor is $1/10$ of that of methyl alcohol. The two alcohols are similar with regard to their critical supersaturation. Therefore in view of the different molecular weights we can assume that the combined concentration of C and O atoms in experiments 3 and 4 is about $1/5$ of the combined concentration in experiments 1, 2, and 5. Table I gives the combined concentrations of C and O atoms calculated for the mean effective height of the sensitive layer.

The quality of the photographs was not greatly impaired by the use of propyl alcohol. However, the vapor diffusion coefficient of this alcohol in hydrogen is smaller by a factor of one and one-half than that of methyl alcohol vapor; this increases the chamber recovery time. Therefore the chamber working cycle was 13 sec in experiments 3 and 4. The registration efficiency for electrons from $\mu \rightarrow e$ decays was 43% in experiments 3 and 4, whereas in experiments 1, 2, and 5 the average was 60%.

All of the approximately 170,000 stereo photographs from experiments 1-5 were scanned twice. An average of one muon ending in the chamber gas was observed in every four photographs (Table I). The scanners selected events resulting from the production of a $d\mu$ atom having some range in the gas. In the photographs these events are observed mainly as the track of a stopping muon along with an electron track displaced from the muon ending, where the electron had resulted from muon decay

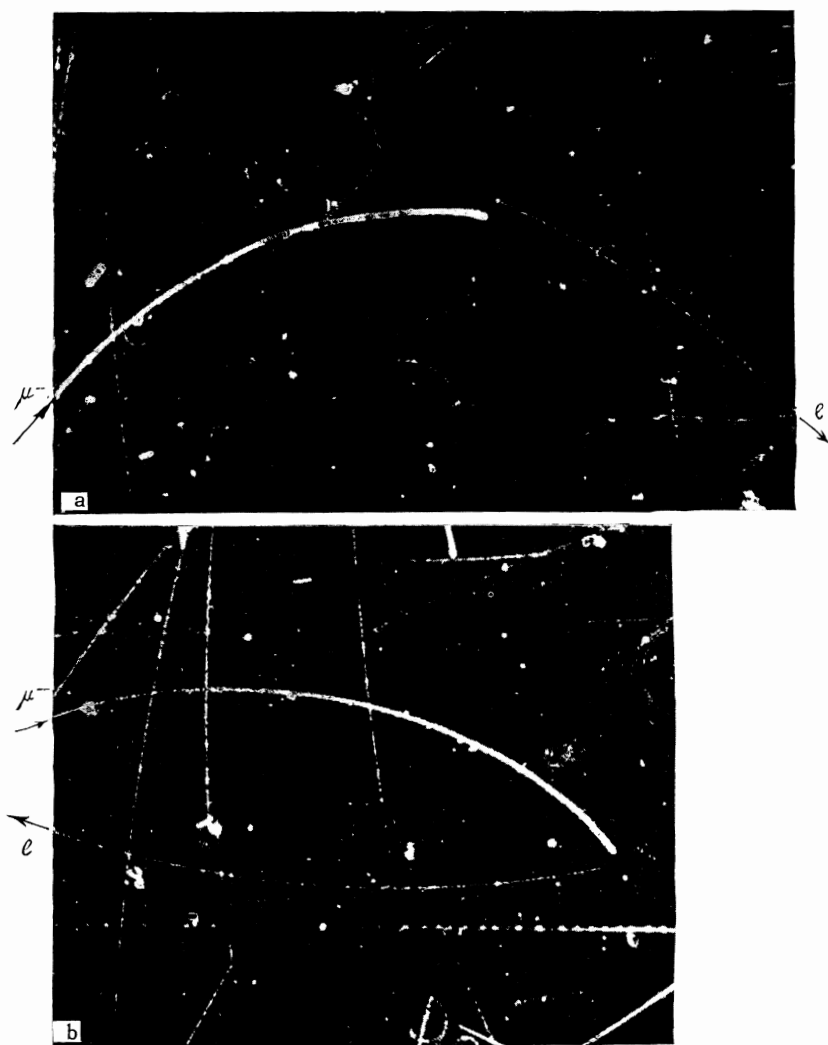


FIG. 2. Photographs of $d\mu$ production. a – Experiment 2 (with methyl alcohol); b – Experiment 3 (with normal propyl alcohol). The range of a $d\mu$ atom is observed as the displacement of a decay-electron track origin from the muon ending. In case a at the origin of the decay-electron track there appears a “dot” which is the track of an Auger electron.

in the orbit of a $d\mu$ or $Z\mu$ atom or of a $pd\mu$ molecule. Events of this type were selected in the photographs from experiments 1, 2, and 3 only when the origin of the electron track showed a clear “dot,” the track of an Auger electron produced in the ground-state transition of a muon from an excited level of a μC or μO atom (Fig. 2a). This selection criterion enables a more exact determination of the $d\mu$ range. Because of the relatively small statistics obtained from experiments 4 and 5, cases were here included without a visible “dot” at the electron track origin (Fig. 2b) but with a clearly determined displacement.¹⁾

The same class of events includes the considerably rarer cases in which $d\mu$ atoms, colliding

with protons or deuterons, form $pd\mu$ and $dd\mu$ mesic molecules, followed by the catalysis of $p+d$ and $d+d$ nuclear fusion reactions; also included are muon transfers from deuterons to complex nuclei with muon capture accompanied by star formation. These events were not used for further study.

All selected events were subject to the requirement that the electron track be clearly visible and that its length exceed 5 mm. Table I gives the number of events in each experiment that were selected in this manner for further measurements.

The selected events were studied under an UIM-22 microscope; the lengths l of $d\mu$ range projections on a horizontal plane were measured (Fig. 3). The accuracy of range measurements (in the object plane) determined by the deviation from the mean when all events were measured twice by a single person, and also in control measurements by a second person, was 0.1 mm.

Since the efficiency of registering $d\mu$ ranges with projection lengths l depends greatly on the

¹⁾The frequency of visible “dots” depends, as in the case of muon transfer from $p\mu$ to complex atoms,[⁴] on the impurity concentration, and is $\sim 70\%$ in experiments 1, 2, and 5 but only $\sim 40\%$ in experiments 3 and 4 because of the smaller transfer probability in the latter.

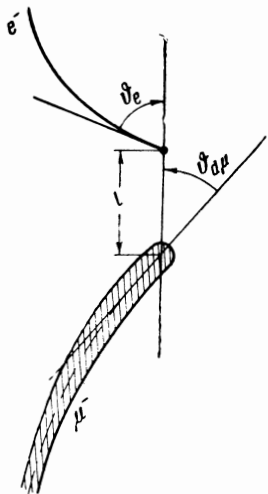


FIG. 3. Schematic drawing of an event showing the $d\mu$ range.

length of l , the following corrections must be taken into account in plotting the range distributions.

1. Since a muon track exhibits considerable width (~ 0.4 mm) near its ending, the registration efficiency can depend on the angular characteristics of the event, i.e., on the angles $\varphi_{d\mu}$ and φ_e (Fig. 3). The angle $\varphi_{d\mu}$ is the projection of the angle between the tangent to the muon track at its ending and the direction of the $d\mu$ atom; the angle φ_e is the projection of the angle between the direction of the mesic atom and the tangent to the decay electron track at the decay point. Both $\varphi_{d\mu}$ and φ_e were measured microscopically to within about 5° . Figure 4 shows the distributions of these angles in the events of experiment 1. Because of the isotropy with respect to space angles, uniform distributions over the angles $\varphi_{d\mu}$ and φ_e should also be found. This is observed in Fig. 4 with respect to the distribution over φ_e ; however, the number of events is reduced for large $\varphi_{d\mu}$. The lower registration efficiency for events in which the $d\mu$ atom moves backward (i.e., $\varphi_{d\mu}$ is close to 180°) is associated with the fact that because of the finite muon track width, these can be regarded as events without a displacement of the electron track origin. This is especially significant for small ranges l , as well as for the registration of events for which a dot is required at the origin of the decay electron track. Therefore for the further analysis of experiments 1–3 only events with $\varphi_{d\mu} < 120^\circ$ were selected. In experiments 4 and 5 the distributions over $\varphi_{d\mu}$ were nearly isotropic and no angle cutoff was required. A correction for angle-dependent registration efficiency is essential only for the smallest values of l ; its average was 12% for $l < 2$ in all experiments.

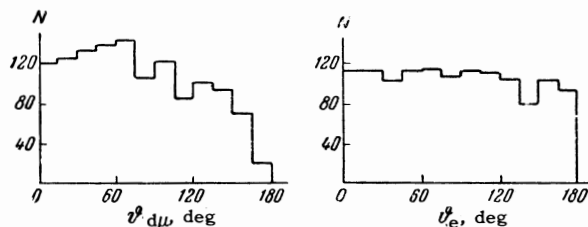


FIG. 4. Distribution of events over the angles $\varphi_{d\mu}$ and φ_e in experiment 1.

2. A correction for the registration efficiency because of the limited sensitive region of the chamber was essential only for large values of l , and was introduced only in the data from experiment 5, where the $d\mu$ range reaches 20 mm because of the low deuterium concentration. The average correction was 10%.

3. A correction for the background of spurious events (when a random particle track close to the muon ending might be considered to be a decay electron track) in experiments 1–4 did not exceed a few percent and was not introduced. For example, Fig. 5 shows the distribution over l in the interval $l = 0$ –10 mm without corrections in experiment 1; it can thus be seen that the background of spurious events is negligibly small for ranges $l = 0$ –5 mm. The correction was 7% for experiment 5, where the ranges are much longer.

The distributions included events with ranges $1 \text{ mm} < l < 5 \text{ mm}$ in experiments 1–4 and $1 \text{ mm} < l < 15 \text{ mm}$ in experiment 5. The last column of Table I shows the final number of events for each experiment in the given intervals after all corrections had been made.

Figure 6 shows the range l distributions; the indicated errors at each point include both the statistical errors and the uncertainty due to the corrections. The numbers of events with ranges $0 < l < 1 \text{ mm}$ in experiments 1, 2, and 4 are also shown.

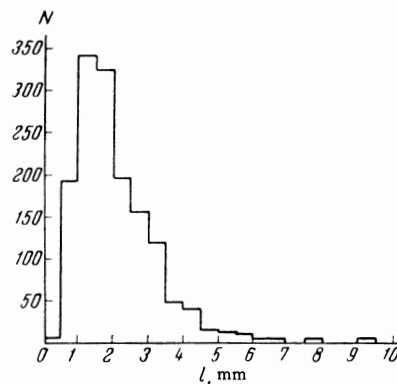


FIG. 5. Distribution of events with respect to $d\mu$ range in experiment 1.

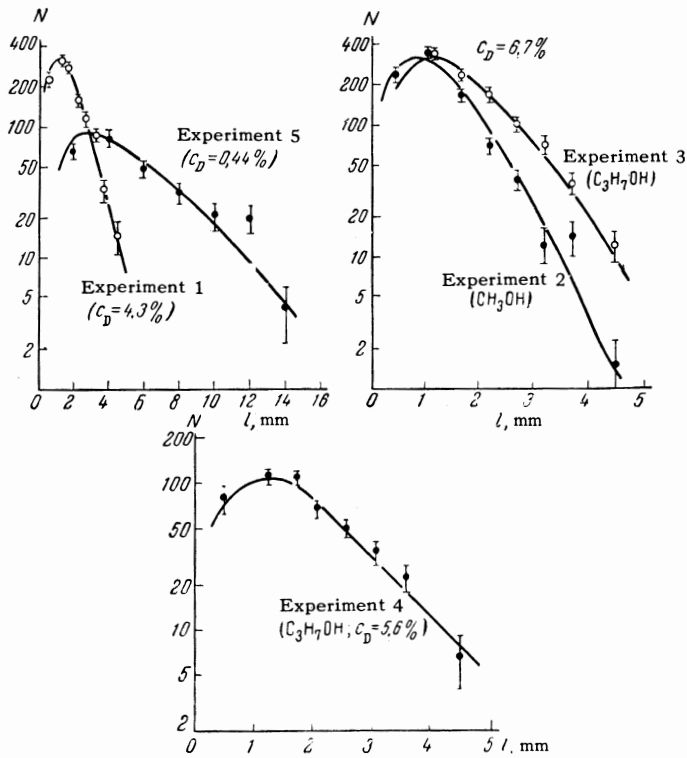


FIG. 6. Experimental distributions of $d\mu$ ranges in experiments 1-5. The curves represent Monte Carlo calculations (see Sec.4) with the parameters given in Table III.

These numbers include both the registered events with visible ranges less than 1 mm and events without visible ranges, the number of which was estimated from the probability of $d\mu$ formation in process (1). These points of the distributions were not included in the further analysis.

We analyzed, in addition to our own experimental distributions, the data obtained by Schiff^[7] using a liquid hydrogen chamber under the experimental conditions given in Table I. The histogram in Fig. 7 represents the $d\mu$ range distribution in the 68 events measured by Schiff.²⁾

3. ANALYSIS OF EXPERIMENTAL DATA

From a qualitative examination of the range distributions obtained with different deuterium concentrations (experiments 1 and 5, Fig. 6) and different C and O concentrations (experiments 2 and 3, Fig. 6) it is seen that with increasing amounts of either deuterium or the Z impurity the distributions are shifted toward smaller ranges. This indicates the relatively strong dependence of the distributions on the macroscopic cross section for

elastic scattering of $d\mu$ atoms on deuterons, $n_d\sigma_{d\mu+d}$ (where n_d is the number of deuterium atoms per cm^3), and the important role of an inelastic process—muon transfer from deuterons to nuclei of higher Z.

The cross sections $\sigma_{d\mu+d}$, $\sigma_{d\mu+p}$, and $\sigma_{d\mu+Z}$ can be obtained quantitatively by using the calculational methods of neutron physics, because the slowing down of $d\mu$ atoms produced in process (1) with the energy 45 eV is analogous in many ways to the slowing of epithermal neutrons in a medium consisting of different nuclei. However, the solution of the kinetic equation describing this process exists in analytic form only for some special cases. In our case the problem was complicated by the additional fact that the $d\mu$ lifetime is comparable to the time required for slowing to thermal velocity, so that the total number of collisions is small (~ 10) and the fraction of collisions in the thermal region is also small. We therefore used the Monte Carlo method to calculate the differential range distributions. The slowing down parameters (cross sections and lifetime) were obtained by comparing the experimental distributions with those calculated by the Monte Carlo method using a χ^2 analysis. An electronic computer was used for all calculations.

The sequence used to simulate the $d\mu$ slowing process and to calculate the ranges is shown in Fig. 8. Only $d\mu$ scattering by deuterons, which, as already mentioned, plays the largest part in the process, was simulated in detail. As is well known from the theory and experimental work on slow neutron scattering in hydrogen, up to neutron

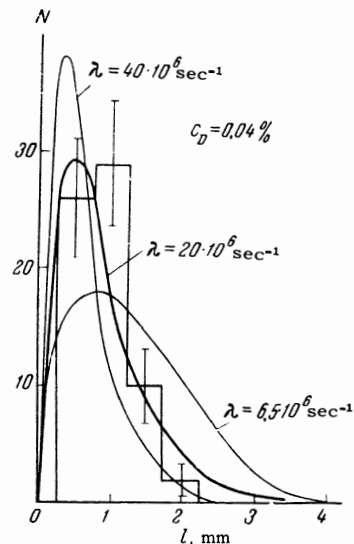


FIG. 7. Schiff's^[7] experimental distributions of $d\mu$ ranges. The curves were calculated by the Monte Carlo method for three different values of λ .

²⁾In this work the $d\mu$ ranges were measured only for events in which stars with visible prongs were observed in the capture of muons by neon nuclei.

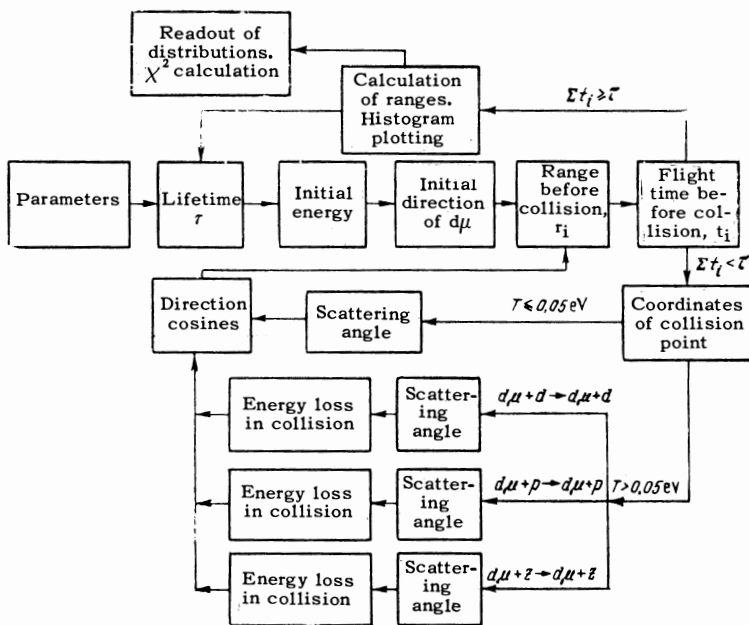


FIG. 8. Simulation of the slowing down of $d\mu$ atoms and the range calculation.

energies of the order of the first molecular vibrational level ($h\nu_{\text{vib}} = 0.4$ eV for D_2 molecules) the scattering can be regarded as taking place on free particles. With further energy decrease molecular bonding exerts an influence as the cross section (per particle in the molecule) increases and small-angle scattering predominates. Our subsequent analysis will show that the l distribution depends very little on the particular hypothesis regarding the character of the interaction for near-thermal energies of the $d\mu$ atoms. Therefore the entire range of $d\mu$ kinetic energy T was divided into only two regions: a) epithermal: 0.05 eV $< T < 45$ eV, and b) thermal (Maxwellian): $T \leq 0.05$ eV.

Scattering on free deuterons was assumed for the epithermal region, with a c.m. isotropic angular distribution. The energy dependence of $\sigma_{d\mu+d}$ was taken from the theoretical work of Cohen et al.,^[2] who showed that the cross section increases by a factor of only 1.5 when the energy changes from 45 eV to 0.05 eV.

For the thermal region it was assumed that the $d\mu$ atoms are scattered elastically by D_2 molecules. In one variant of the calculation the cross section in the thermal region was taken to be constant and 1.5 times greater than $\sigma_{d\mu+d}^T$ at the limit 0.05 eV; in other variants the cross section at the limit was assumed. It was also assumed that collisions in the thermal region occur with D_2 molecules at rest. The Maxwellian distribution for D_2 was used only in calculating the mean energy of relative motion of $d\mu$ atoms and D_2 molecules, which is 0.045 eV at 242°K (our experimental condition). The angular distribution of scattered $d\mu$

atoms was taken to be either isotropic in the c.m. system, or to have the form derived by Schwinger and Teller^[8] for neutron scattering by H_2 molecules. Taking the mass difference between the deuteron and proton into account, we have

$$\frac{d\sigma}{d\Omega} \sim \left[\sin\left(2.5 \sin \frac{\theta}{2}\right) / 2.5 \sin \frac{\theta}{2} \right]^2. \quad (5)$$

This is the distribution for $d\mu$ scattering at 0.045 eV by D_2 in the ground state.

In view of the weak influence of the macroscopic cross sections $n_p\sigma_{d\mu+p}$ and $n_Z\sigma_{d\mu+Z}$ on the range distributions, it was assumed that the $d\mu$ atoms are scattered by free protons and C or O nuclei. The angular distributions of $d\mu + p$ and $d\mu + Z$ scatterings were taken to be isotropic with scattering cross sections that are independent of energy in the entire energy range.

The calculational program included the kinematic dependences for each type of scattering, as well as the angular and energy dependences of the scattering cross sections. The macroscopic cross sections in each experiment were given as proportional to the concentration of the appropriate nucleus. The $d\mu$ lifetime $\tau = 1/\lambda$ used for experiments 1, 2, and 5 was one-third of the value used for experiments 3 and 4, i.e., $\lambda = \frac{1}{3}\lambda_1 = \frac{1}{3}\lambda_2 = \lambda_3 = \lambda_4 = \frac{1}{3}\lambda_5$.³⁾ It was assumed in all instances that the $d\mu$ lifetime is independent of its velocity.

³⁾This ratio was determined from the combined yield of the reactions $d\mu + p \rightarrow \text{He}^3 + \mu^-$ and $d\mu + d \rightarrow t + p + \mu^-$, which was 3.0 ± 0.8 times larger for propyl alcohol than for methyl alcohol.

We also calculated the distribution under the conditions of Schiff's experiment,^[7] in which the elastic scattering of $d\mu$ atoms by protons plays an appreciable part. We used here the value $\lambda = 2 \times 10^7 \text{ sec}^{-1}$, which was obtained from data on the probabilities of mesic molecule $pd\mu$ production and muon transfer to neon nuclei in liquid hydrogen.^[9,10] The small contribution of the cross section $\sigma_{d\mu+p}$ determined by analyzing this distribution was taken into account in calculating the distributions in experiments 1–5.

In the course of the calculation we also obtained for each experiment the mean number of elastic collisions and the mean $d\mu$ velocity, given by

$$\bar{q} = \frac{1}{M} \sum_m q_m, \quad \bar{v}_{d\mu} = \frac{\sum_{i,m} (r_i)_m}{\sum_{i,m} (t_i)_m}, \quad (6)$$

where r_i is the distance traversed by a mesic atom between its i -th and $(i+1)$ -st collisions, t_i is the flight time between these collisions, the subscript m numbers the mesic atom, and M is the number of Monte Carlo (random sample) events. In order to reduce the statistical errors in the calculated distributions, the number of Monte Carlo events for each experiment exceeded by about one order of magnitude the number of events in the experimental distributions.

The Monte Carlo calculational program was tested on the calculation of several variants of the ordinary diffusion problem. The distributions obtained in this way agree well with the exact analytic solution of this problem.

The parametric values which best describe the experimental range distributions were obtained by minimizing the functional

$$\chi^2 = \sum_{k=1}^5 \sum_{j=1}^7 \frac{(N_{k,j}^{\text{exp}} - N_{k,j}^{\text{calc}})^2}{\Delta_{k,j}^2 + \delta_k N_{k,j}^{\text{calc}}}, \quad (7)$$

where $N_{k,j}^{\text{exp}}$ is the number of events in the j -th interval ($j = 1, 2, \dots, 7$) for experiment k ($k = 1, 2, \dots, 5$); $N_{k,j}^{\text{calc}}$ is the number of events in the j -th interval of the distribution calculated by the Monte Carlo method for experiment k , normalized to the total number of events in the experimental distribution for experiment k :

$$N_k^{\text{exp}} = \sum_{j=1}^7 N_{k,j}^{\text{exp}};$$

$\Delta_{k,j}$ is the error in the experimental number of events, $N_{k,j}^{\text{exp}}$; $\delta_k N_{k,j}^{\text{calc}}$ takes into account the statistical spread of the calculated distributions ($\delta_k = N_k^{\text{exp}}/M_k$, and M_k is the total number of Monte Carlo events for experiment k). The minimum of

the functional (7) was obtained by variation of the parameters λ , $\sigma_{d\mu+d}$, and $\sigma_{d\mu+Z}$ using the linearization method.^[11] Because of the well fulfilled quadratic character of the functional (7) at its minimum, only three or four iterations were required to arrive at the minimum.

4. RESULTS OF THE ANALYSIS

The experimental and calculated distributions of l are compared in Tables II and III. Table II gives the parameters for the minimum of χ^2 and the values of χ_{min}^2 for three variants characterized by different hypotheses regarding $d\mu$ scattering by deuterons in the thermal energy region. It is seen that the smallest value $\chi_{\text{min}}^2 = 37$, when 32 is expected (for 35 experimental points and 3 variable parameters) is reached for variant C, which was based on the hypothesis that the cross section for $d\mu+d$ scattering does not change for T_{therm} and that the angular distribution for T_{therm} has the form (5). Table III gives the parameters for each experiment in this variant; the curves in Fig. 6 were calculated using these parameters.

Table II shows the very good agreement with experiment in the cases of the other two variants ($\chi_{\text{min}}^2 = 42$ and 41) and that the values of the parameters are close for all three variants. This results from the fact that in the thermal region the mesic atoms have low velocities and undergo relatively few collisions. Table III gives the mean velocity $\bar{v}_{d\mu}$ of $d\mu$ atoms and the mean number \bar{q} of collisions for each experiment. It can be seen that \bar{q} exceeds the mean number (10) of collisions before slowing down only in experiments 3 and 4, where the mesic atom lifetime τ is relatively long.

Since the mean velocity for each experiment exceeds the thermal velocity $2 \times 10^5 \text{ cm/sec}$, we conclude that complete thermalization was attained in none of these experiments. In experiment 3, where about five collisions occurred in the thermal region, it was considered that $d\mu$ atoms collide with D_2 molecules having a Maxwellian velocity distribution. Figure 9 shows the close curves obtained with and without allowance for the Maxwellian distribution.

The contribution of the macroscopic cross sections for scattering by protons and complex nuclei (Table III) is small for experiments 1–4, and is comparable to the contribution of the macroscopic cross section for scattering by deuterons in experiment 5. In calculating the distribution for Schiff's experiment, because of the small number of exper-

Table II

Variant*	Angular distribution (c.m. s.)	$\sigma_{d\mu+d}$	Parameters** for minimum of χ^2				χ^2_{min}	$\chi^2_{min}/\bar{\chi}^2$
			$n_d \sigma_{d\mu+d}$, cm^{-1}	$n_p \sigma_{d\mu+p}$, cm^{-1}	$n_z \sigma_{d\mu+z}$, cm^{-1}	λ , 10^6sec^{-1}		
A	Isotropic	$\sigma_{d\mu+d}^r$	35.3 ± 0.6	$1.0^{+1.0}_{-0.5}$	1.8 ± 0.2	0.76 ± 0.03	42	1.31
B	From (5)	$1.5 \sigma_{d\mu+d}^r$	34.8 ± 0.8					
C	From (5)	$\sigma_{d\mu+d}^r$	35.2 ± 0.6					

*For $T < T_{\text{therm}}$.

**This table gives the macroscopic cross sections for experiment 3. The cross sections for the other experiments can be obtained using the ratios of the d and Z nuclear concentrations in these experiments.

Table III

Experiment	Parameters for minimum of χ^2				$\bar{v}_{d\mu}$, 10^6cm/sec	Mean number of collisions	Number of Monte Carlo events	Reproducibility of χ^2		
	$n_d \sigma_{d\mu+d}$, cm^{-1}	$n_p \sigma_{d\mu+p}$, cm^{-1}	$n_z \sigma_{d\mu+z}$, cm^{-1}	λ , 10^6sec^{-1}				Calculation 1	Calculation 2	Calculation 3
1	22.6	1.0	1.80	2.43	5.8	8.1	7000	11.4	11.6	11.7
2	35.2	1.0	1.80	2.43	4.7	9.2	5000	10.8	10.9	11.0
3	35.2	1.0	0.36	0.81	3.0	15.3	7000	3.5	3.4	3.7
4	29.0	1.0	0.36	0.81	3.2	13.7	3000	2.7	2.6	2.8
5	2.5	1.0	1.80	2.43	15.2	5.8	3000	8.5	8.1	8.4
From [7]	0	30.0	0	20.0	17.5	4.7	1000	—	—	—
Σ							26000	36.9	36.6	37.6

imental events and the somewhat uncertain value of λ the contribution of the macroscopic cross sections for scattering by deuterons and neon nuclei was neglected, scattering only by protons being assumed. The heavy curve in Fig. 7 represents a Monte Carlo calculation of the distribution for $\lambda = 2 \times 10^7 \text{sec}^{-1}$ and $n_p \sigma_{d\mu+p} = 30 \text{cm}^{-1}$. The dependence of the calculated distributions on λ can be seen from the curves in this figure. The number of Monte Carlo events and the value of χ^2 for each experiment are given in Table III. The values of χ^2 were reproduced within 1.5% when recalculated using different random numbers.

The errors indicated in Table II for the macro-

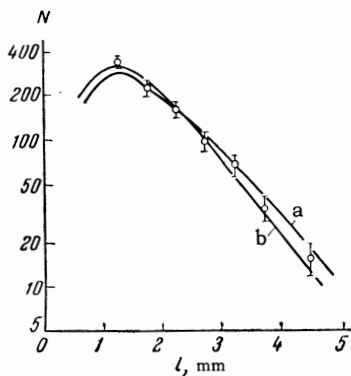


FIG. 9. Calculated $d\mu$ range distributions for experiment 3 (a) with and (b) without allowance for Maxwellian velocities of D_2 molecules, compared with experimental results.

scopic cross sections and λ , as calculated by means of linearization, are somewhat too low, because, as already mentioned, the calculated distributions have some statistical spread. For our final results we used the parameter errors determined from the condition $\chi^2 = \chi^2_{\text{min}} + 1$. Table IV gives the final cross sections for elastic $d\mu$ scattering. The errors indicated for $\sigma_{d\mu+d}$ and $\sigma_{d\mu+z}$ include uncertainties in the assumed deuterium concentration and in the estimated C and O contents.

5. DISCUSSION OF RESULTS

In addition to the experimental cross sections, Table IV gives the theoretical cross sections calculated in [3,2]. According to these investigations the $d\mu+d$ scattering at low energies is s scattering to a very good approximation; by analogy with neutron scattering the cross section can be represented at $T = 0$ by ⁴⁾

$$\sigma_{d\mu+d} = 4\pi(2/3a_g^2 + 1/3a_u^2), \quad (8)$$

where a_g and a_u are the scattering lengths for the

⁴⁾It should be noted that the experimental value of the cross section for $d\mu+d$ scattering pertains to the effective energy $T = 0.1 \text{eV}$, and because of its very slight energy dependence it can be identified with $\delta_{d\mu+d}$ for $T = 0$, the calculated values of which are given in Table IV.

Table IV

Process	Cross section for elastic $d\mu$ scattering, cm^2	
	Experimental	Theoretical
$d\mu + d \rightarrow d\mu + d$	$(4.15 \pm 0.29) \cdot 10^{-19}$	$3.3 \cdot 10^{-19}$ [3] $3.5 \cdot 10^{-19}$ [2]
$d\mu + p \rightarrow d\mu + p$	$(0.8^{+0.8}_{-0.4}) \cdot 10^{-21}$	$\sim 10^{-21}$ [2]
$d\mu + Z \rightarrow d\mu + Z$	$(1.2 \pm 0.3) \cdot 10^{-18}$	$\sim 10^{-18}$

mesomolecular potentials V_g and V_u corresponding to nuclear repulsion and attraction. For identical nuclei the approximation of the potentials and the determination of the scattering lengths are somewhat simplified and are performed in the customary adiabatic approximation corrected mainly for muon motion in the mesic atom. For $d\mu$ scattering (unlike the scattering of $p\mu$ atoms by protons which we studied in [4]) the cross section (8) is practically independent of the $d\mu$ spin state (the total spin of a $d\mu$ atom can be $\frac{3}{2}$ or $\frac{1}{2}$). This is associated with the fact that the scattering lengths a_g and a_u have identical signs and are almost equal in magnitude [12] (according to [3], $a_g = 6.67$ and $a_u = 5.76$ in units of $\hbar^2/m_\mu e^2 = 2.56 \times 10^{-11}$ cm). The good agreement between the two theoretical calculations of the cross section $\sigma_{d\mu+d}$ [2,3] and their agreement with experiment provide justification for the approximations used in the theory.

The experimental value of $\sigma_{d\mu+p}$ given in Table IV was obtained by analyzing the distribution in an experiment with liquid hydrogen. [7] An analysis employing only our own data (experiments 1–5) yielded the result $\sigma_{d\mu+p} < 5 \times 10^{-21} \text{ cm}^2$. According to the theoretical calculations in [2] elastic $d\mu+p$ scattering can involve the Ramsauer-Townsend effect. In this case low-energy scattering depends only on the s phase, and the cross section vanishes when the laboratory energy of the $d\mu$ atom is about 0.45 eV (Fig. 10). This effect is derived from the consideration of long-range forces in the scattering potential at distances greater than 20 Bohr radii of the muon. It was also shown in [2] that when these long-range forces are neglected the cross section is $5.3 \times 10^{-21} \text{ cm}^2$ and is almost energy-independent. The experimental cross section pertains to an effective energy $T \sim 1$ eV and agrees qualitatively with the assumed presence of the Ramsauer-Townsend effect.

Our present analysis also furnished independent information regarding the $d\mu$ lifetime in hydrogen gas. In experiments 3 and 4 with normal propyl alcohol, when the concentration of C and O nuclei was about 1/4000 this lifetime was close to the muon lifetime. The combined rate of inelastic processes in these experiments is $\lambda = \lambda_0 + \lambda'_{ZCZ}$

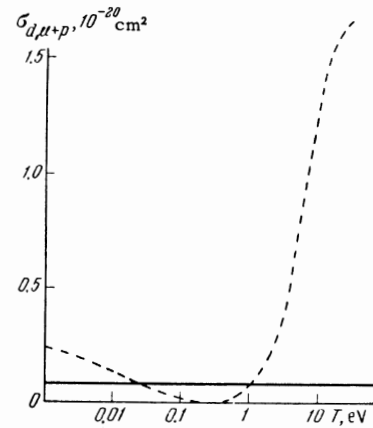


FIG. 10. Cross section for elastic scattering of $d\mu$ atoms by protons versus laboratory kinetic energy of the mesic atoms. Dashed curve - according to [2]; solid line - relation used in present calculation.

+ $\lambda'_{pd\mu} = (0.8 \pm 0.1) \times 10^6 \text{ sec}^{-1}$. For experiments 1, 2, and 5 we have $\lambda = (2.4 \pm 0.3) \times 10^6 \text{ sec}^{-1}$. From this last result, with a small correction ($\sim 3\%$) for the formation of $pd\mu$ molecules in the gas, it follows that the rate of muon transfer from $d\mu$ atoms to C and O nuclei is

$$(\lambda'_Z C_Z)^d = (1.9 \pm 0.3) \cdot 10^6 \text{ sec}^{-1}, \quad (9)$$

which is the mean rate of transfer to carbon and oxygen. Using the results obtained in [4,5] for the transfer rate to C and O from $p\mu$ atoms, we obtain the ratio

$$\frac{(\lambda_Z C_Z)^d}{(\lambda'_Z C_Z)^p} = \frac{(1.9 \pm 0.3) \cdot 10^6 [\text{sec}^{-1}]}{(0.9 \pm 0.25) \cdot 10^6 [\text{sec}^{-1}]} = 2.1 \pm 0.7.$$

This ratio is insensitive to uncertainty regarding the impurity concentration, because the compared experiments were performed under identical conditions. After converting to the density of liquid hydrogen, Eq. (9) becomes

$$\lambda_{C, O}^d = (4.7 \pm 1.4) \cdot 10^{10} \text{ sec}^{-1},$$

which agrees qualitatively with the rate of muon transfer from $d\mu$ to neon ($Z = 10$), for which the measured rate in liquid hydrogen is $1 \times 10^{11} \text{ sec}^{-1}$. [7,9,10] We note that the theoretical value of the transfer rate to oxygen is close to $5 \times 10^{10} \text{ sec}^{-1}$. [13]

The cross section σ_Z for the transfer of a muon from a deuteron to a carbon or oxygen nucleus can be determined from the relation $\lambda'_Z = n_Z \sigma_Z \bar{v}_{d\mu}$ and has the value $0.8 \times 10^{-18} \text{ cm}^2$ under the conditions of experiment 5. The elastic scattering cross section $\sigma_{d\mu+Z}$ agrees with this value (Table IV), which was to be expected since $\sigma_{d\mu+Z} \geq \sigma_Z$.

In conclusion it must be mentioned that an analy-

sis similar to the foregoing is being performed at the present time for the scattering of $p\mu$ atoms by protons. Our present results are also important for interpreting the yields of the nuclear reactions $p + d\mu \rightarrow He^3 + \mu^-$ and $d\mu + d \rightarrow t + p + \mu^-$, data for which will be published later.

The authors are deeply indebted to S. S. Gershtein, Yu. M. Kazarinov, I. N. Silin, R. M. Sulyaev, and V. M. Tsupko-Sitnikov for valuable discussions and comments, and to L. I. Krasnoslobodtseva, Yu. L. Saikina and T. S. Ob'ezdnova for assistance with the measurements.

¹ Alvarez, Bradner, et al., Phys. Rev. **105**, 1127 (1957).

² Cohen, Judd, and Riddell, Phys. Rev. **119**, 397 (1960).

³ Ya. B. Zel'dovich and S. S. Gershtein, UFN **71**, 581 (1960), Soviet Phys. Uspekhi **3**, 593 (1961).

⁴ Dzhelepov, Ermolov, Kushnirenko, Moskalev, and Gershtein, JETP **42**, 439 (1962), Soviet Phys. JETP **15**, 306 (1962).

⁵ Dzhelepov, Friml, Gerstein, Katyshev, Moskalev, and Yermolov, Proc. of the 1962 International Conference on High Energy Physics at CERN, p. 484; V. P. Dzhelepov, Atomnaya énergiya **14**, 27 (1963),

⁶ Dzhelepov, Ermolov, Katyshev, Moskalev, Fil'chenkov, and Friml, Preprint D-1551, Joint Inst. for Nuclear Research, 1964.

⁷ M. Schiff, Nuovo cimento **22**, 66 (1961).

⁸ J. Schwinger and E. Teller, Phys. Rev. **52**, 286 (1937).

⁹ Conforto, Focardi, Rubbia, and Zavattini, Phys. Rev. Letters **9**, 432 and 525 (1962).

¹⁰ Anderson, Bleser, Lederman, Meyer, Rosen, Rothberg, and Wang, Phys. Rev. **132**, 2679 (1963).

¹¹ S. N. Sokolov and I. N. Silin, Preprint D-810, Joint Inst. for Nuclear Research, 1961.

¹² S. S. Gershtein, JETP **40**, 698 (1961), Soviet Phys. JETP **13**, 488 (1961).

¹³ S. S. Gershtein, JETP **43**, 706 (1962), Soviet Phys. JETP **16**, 501 (1963).

Translated by I. Emin